Change of electronic structures with carrier doping in the highly correlated electron system $Y_{1-x}Ca_xTiO_3$

Y. Taguchi, Y. Tokura,* T. Arima, and F. Inaba
Department of Physics, University of Tokyo, Tokyo 113, Japan
(Received 23 December 1992)

A perovskitelike solid solution $Y_{1-x}Ca_xTiO_3$ can be viewed as a hole-doped Mott-Hubbard insulator or strongly correlated metal that is derived from the parent insulator $YTiO_3$ with the Mott-Hubbard gap of ~ 1 eV. The Mott insulator-metal transition is observed around the hole-doping level of $x \sim 0.35$ in $Y_{1-x}Ca_xTiO_x$. Change of electronic structures with hole doping has been investigated by measurements of optical spectra in a wide photon-energy range. In the insulating phase with $x < 0.4$, the spectral weight is transferred from the Mott-Hubbard gap excitations to the inner-gap region with hole doping, giving rise to a gradual closing of the charge gap. Even in the doping-induced metallic region ($x \geq 0.4$), the midinfrared absorption still dominates the lower-lying Drude absorption, perhaps due to the effects of the impurity potential and electron correlation on the narrow $3d$. band. The results were argued in comparison with the case of the high-T_c cuprates.

I. INTRODUCTION

The $Ti^{3+}(3d^1)$-based oxides are mostly insulating or barely metallic due to strong electron-correlation effects in the relatively narrow $3d$ electron bands. The ternary compound $RTiO_3$, where R is a rare-earth element, is a prototypical example for the Mott-Hubbard insulator with localized half spins.[1-4] The system we have investigated in this work is the Mott-Hubbard insulator $YTiO_3$ and its hole-doped analogs $Y_{1-x}Ca_xTiO_3$ with a perovskitelike lattice structure. With use of such a hole-dopable Mott insulator, we have spectroscopically investigated a change of electronic structures as the system undergoes the insulator-metal transitions.

The hole-doping-induced change of the electronic structure in the correlated insulator is also an important issue in the study of the normal-state properties of high-T_c superconducting cuprates. According to the Zaanen-Sawatzky-Allen scheme,[5] the parent cuprate compounds with the $3d^9$ (i.e., $3d^1$ hole) configuration may be classified as the charge-transfer (CT) insulator where the charge gap is formed between the occupied O $2p$ states and unoccupied Cu $3d_{x^2-y^2}$ states (upper Hubbard band). By contrast, the parent titanate insulators with the $3d^1$ configuration is a Mott insulator (in a narrow sense) in which the minimum charge gap is formed between the correlated $3d$ states (lower and upper Hubbard bands). In this sense, experimental investigations on electronic structures in hole-doped Mott insulators like $Y_{1-x}Ca_xTiO_3$ will be important also from a viewpoint of comparison with the case of hole- (or electron-) doped CT insulators such as cuprate superconductors. In particular, change of the optical spectra with carrier doping in such a correlated electron system is also of particular interest in relation to the problem of the so-called "inner-gap states" in cuprate superconductors: It has been spectroscopically observed in the layered cuprate compounds that the new state (inner-gap state) is formed near the Fermi level and within the original CT gap with hole or electron doping.[6-10] In fact, we have observed in the present study a similar midinfrared band in the nominally hole-doped samples, $Y_{1-x}Ca_xTiO_3$, which will be argued in comparison with the case of the doped cuprates.

The parent insulator $YTiO_3$ is one of the family of the perovskitelike rare-earth titanates $RTiO_3$ where the trivalent A site ($=R$) can be any of rare-earth ions from La to Lu.[1-3] (An exception is $EuTiO_3$ in which Eu is divalent.) Within the family of $RTiO_3$, the electrical and magnetic properties seem to depend critically but systematically on the ionic radius of R^{3+} ion or equivalently on the tolerance factor of the compound.[2] The $RTiO_3$ crystal can be viewed as an orthorhombically distorted perovskite structure (so-called $GdFeO_3$-type structure) where the TiO_6 octahedron tilts alternatingly. The Ti-O-Ti bond angle in $RTiO_3$ shows a deviation from 180°; for example, 157° (along the ab plane) and 158° (along the c axis) in $LaTiO_3$ and 140° and 144° in $YTiO_3$.[11] Such a tilting of the TiO_6 octahedron affects the one-electron bandwidth of the $3d$ electron, since the hopping interaction is dominated by a supertransfer interaction via the oxygen $2p$ states. Reflecting the situation, $LaTiO_3$ with a relatively weak effect of electron correlations is an antiferromagnetic insulator with T_N around 140 K (Refs. 2, 4, and 12–14) and show the Mott-Hubbard gap of ~ 0.1 eV.[12] On the other hand, $YTiO_3$ with a narrower $3d$ bandwidth is a ferromagnetic insulator with T_c around 30 K (Refs. 2, 13, and 14) and its Mott-Hubbard gap is ~ 1 eV (as observed in the present study). Variation of the magnetic properties appears to be a continuous function of the tolerance factor or the bandwidth of the $3d$ electrons as demonstrated by the studies of the magnetic properties in $RTiO_3$ with varying R species[2] and also in the solid solution system $(La,Y)TiO_3$.[14] The ferromagnetic ground state in the case of the relatively strong electron correlation likely arises from the orbital

(pseudo) degeneracy in $3d$ t_{2g}-like states. The real crystal suffers from the orthorhombic distortion, yet a shape of the TiO_6 octahedron remains to be nearly undistorted and hence the crystal-field splitting of the t_{2g} states will be much smaller than the intra-atomic exchange interaction (Hund's coupling energy). Therefore, the system $RTiO_3$ and their hole-doped analogs may be better described theoretically by a degenerate (multiband) Hubbard model rather than by a single-band Hubbard model.

In the solid solution system $Y_{1-x}Ca_xTiO_3$, we can control the effective Ti valence from $3+(x=0)$ to $4+(x=1)$, which drives the system from a Mott-Hubbard insulator ($YTiO_3$) with $3d^1$ configuration to a band insulator ($CaTiO_3$) with no $3d$ electron. Such an A-site substitution with a different valence element is the most effective way for controlling the B-site (Ti) valence or the band filling, while keeping the fundamental Ti-O network. Another good example for a success in such a valence control is the case of single CuO_2-layered cuprate superconductor,[15] e.g., $La_{2-x}Sr_xCuO_4$ (hole doped) and $Nd_{2-x}Ce_xCuO_4$ (electron doped). $Y_{1-x}Ca_xTiO_3$ in the low-x region can be viewed as hole doped in the parent insulator $YTiO_3$ by a partial substitution of Y^{3+} sites with Ca^{2+} ions. Such a hole-doping procedure drives, in general, the phase change from a Mott-Hubbard insulator to a correlated metal. In the high-x region, on the other hand, the picture of electron doping in the band insulator ($CaTiO_3$) may be better, since the $3d$ band is continuously filled up from the bottom with the filling parameter $n=1-x$. In fact, we have observed a transitional behavior from the doped Mott insulator to the narrow band metal with increasing x (or decreasing the filling n).

II. EXPERIMENT

A. Sample preparation

All the samples investigated were melt grown by a floating-zone method. First, powder of Y_2O_3 and TiO_2 was dried at 900 °C in air for 12 h. Then, the end compounds, $CaTiO_3$ and $YTiO_3$, were prepared in form of ceramics, which were used as sources of the solid solutions: $CaTiO_3$ was prepared by calcining the mixture of $CaCO_3$ and TiO_2 in an alumina crucible in air at 1100 °C after regrinding and pressing the precalcined ingredient. On the other hand, slightly oxygen-deficient mixture ($YTiO_{2.97}$) of Y_2O_3, Ti, and TiO_2 was pressed into a bar and heated in a vacuum (less than 10^{-2} Torr) at 1500 °C for 30 min. Ground mixture of $YTiO_3$ and $CaTiO_3$ with a prescribed ratio (x) was pressed into a rod with a size of 5 mm $\phi\times 40$ mm and loaded in a floating-zone furnace equipped with two halogen lamps and double hemielliptic focusing mirrors.

Over the whole concentration x, the ingredient could be melted congruently. Crystals were melt grown in a reducing atmosphere; in a flow of gas mixture, Ar 60%/H_2 40% for $x=0$ ($YTiO_3$) and 100% Ar ($6N$ purity) for $x=0.1-0.9$. In order to avoid a possible gradient effect in passing the melted zone, the feeding speed was set rather high, at 60 mm/h except for the case of $YTiO_3$ (5 mm/h).

Measurements of powder x-ray diffraction showed that the obtained compounds were of a single phase. The crystal structure is perovskitelike with an orthorhombic distortion ($GdFeO_3$-type) over the whole composition region from $x=0$ ($YTiO_3$) to $x=1$ ($CaTiO_3$). Figure 1 shows a variation of the lattice constants with x. Note that the unit-cell lengths, **a**, **b**, and **c**, in the orthorhombic setting are approximately $\sqrt{2}\mathbf{a}_p$, $\sqrt{2}\mathbf{a}_p$, and $2\mathbf{a}_p$, $\mathbf{a}_p$ being the unit-cell length of the cubic perovskite structure. There is no discernible jump of lattice parameters as a function of x, ensuring a continuous formation of the solid solution over the whole composition region. We have assumed the pseudocubic symmetry in analyzing the spectroscopic data for the solid solution, since anisotropic effect is considered not to be significant within the experimental accuracy that the spectroscopic study can attain.

Thermogravitation analysis showed that nonstoichiometry of the sample was fairly small. For example, the composition of the $x=0$ insulator was determined to be $YTiO_{3.03}$ assuming the oxygen nonstoichiometry. Furthermore, it has also been known for the analogous $(La,Sr)TiO_3$ system[16,17] that the oxygen nonstoichiometry is usually less than 0.03 when the sample is prepared with a precise starting mixture of the prescribed ratio (including oxygen content) and in inert (e.g., Ar) atmosphere. Apart from the end $YTiO_3$ compound where a stronger reducing condition is necessary to minimize the oxygen nonstoichiometry, all the solid solution samples were grown in the same atmosphere (i.e., in a flow of Ar gas). Therefore, a slight (and perhaps systematic even if any) deviation of oxygen stoichiometry will not be serious, as far as the present spectroscopic investigation for the insulator-metal transition is concerned.

To characterize the compounds, we have measured temperature dependence of resistivity and magnetic susceptibility for each sample. For four-probe resistivity measurements, the sample was cut to a rectangular shape, typically $3\times 1\times 0.5$ mm^3. Electrical contacts were made

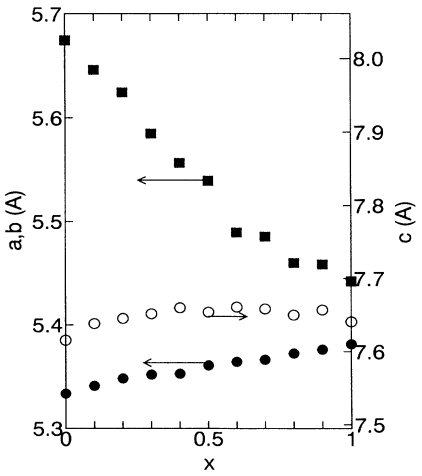

FIG. 1. Lattice constants in $Y_{1-x}Ca_xTiO_3$.

with indium for $x \geq 0.4$ and copper paste for $x \leq 0.3$. Measurements of magnetic susceptibility were carried out with a superconducting quantum interference device magnetometer with application of magnetic field of 1 T. To determine a critical temperature for the ferromagnetic transition in the low-x samples, the magnetization was also measured with a low field (10 mT).

B. Optical measurements

Optical reflectivity measurements were done for the photon-energy range between 7.5 meV and 30 eV on specularly polished surfaces of the samples. No grain boundary was discernible between the single crystalline domains (perhaps of sub-mm size) on the polished surface of the sample by a visual inspection under an optical microscope. In the photon-energy range between 7.5 meV (60 cm^{-1}) and 0.75 eV (6000 cm^{-1}), a Fourier transform spectrometer was used. The reflectivity above 0.5 eV (4000 cm^{-1}) was obtained by a grating spectroscopy. As a light source in the vacuum-ultraviolet region (>6 eV), we utilized a synchrotron radiation at INS-SOR, Institute for Solid State Physics, University of Tokyo. Spectra of the optical conductivity were obtained by the Kramers-Kronig analysis with the following extrapolation procedures: For the metallic samples for $0.4 \leq x \leq 0.8$, the far-infrared reflectivity $R(\omega)$ below 7.5 meV was extrapolated by the Hagen-Rubens relation, $1-R(\omega) \propto \sqrt{\omega}$, whereas the constant reflectivity was assumed for the other samples. For the higher-energy reflectivity above 28 eV, we applied the Drude extrapolation, $R(\omega) \propto \omega^{-4}$.

III. INSULATOR-METAL TRANSITION WITH HOLE DOPING

In Fig. 2 we show the temperature dependence of the resistivity (ρ) in $Y_{1-x}Ca_xTiO_3$. $YTiO_3$ shows a typically insulating behavior with a thermal activation energy of ~ 220 meV. The hole-doping procedure by substitution of Y sites with Ca decreases the resistivity, yet the system remains insulating or semiconducting up to $x=0.3$. For the $x=0.3$ and 0.35 sample, ρ reaches the maximum around 100 and 150 K, respectively, and then rather tends to decrease with lowering temperature. Resistivity in these samples shows hysteresis against temperature, indicating that the reentrant behavior of resistivity is due to an intrinsic phase change coupled with lattice degree of freedom. Details of this temperature-induced phase transition in such a narrow composition region as close to the insulator-metal phase boundary will be discussed in a separate publication and let us concentrate here on an overall feature of the doping-induced phase transition.

The $x=0.4$ sample clearly shows a metallic behavior, in which ρ increases very rapidly with temperature up to 200 K with a saturating tendency at higher temperatures. At $x=0.5$, the minimum resistivity ($\sim 4\times 10^{-4}$ Ω cm at 300 K) was attained. For $0.4 \leq x \leq 0.7$, the metallic resistivity below 30 K shows quadratic dependence on temperature, such as $\rho-\rho_0 \propto T^2$ (ρ_0 being a residual resistivity). The behavior is reminiscent of the electron-electron scattering process in a strongly correlated metal. With

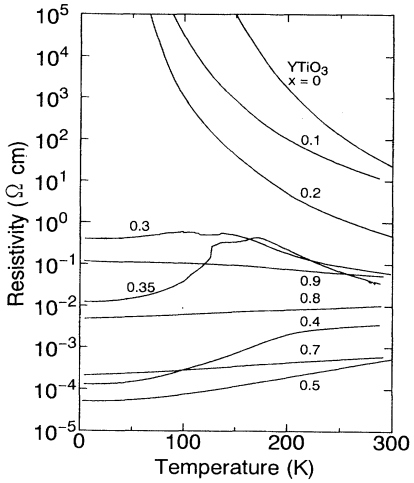

FIG. 2. Temperature dependence of resistivity in $Y_{1-x}Ca_xTiO_3$.

further increase of x, the resistivity rather increases perhaps due to a decrease in density of electron-type carriers (approximately $n=1-x$ per Ti site). The $x=0.9$ sample behaves like a doped semiconductor, which may be ascribed to a poor shielding effect of the impurity (Y site) potential by a low density of carriers.

Temperature dependence of the magnetic susceptibility χ is shown in Fig. 3. The data were corrected for a diamagnetic contribution from the ionic cores. As seen in Fig. 3(a), the strongly temperature-dependent susceptibility was observed for $x \leq 0.35$, indicating the presence of almost localized moments on Ti sites. By contrast, χ in the metallic compounds with $x \geq 0.4$ show a nearly temperature-independent behavior (except for the low-temperature increase in the $x=0.4$ sample), being typical of the Pauli paramagnetism. The magnitude of χ_{Pauli} is expected to be proportional to the density of states at the Fermi level (E_F) in the simple metal scheme, which would be proportional to $n^{1/3}$ (n being the d-band filling; $n=1-x$) in the parabolic band. However, the observed χ values in the metallic region ($0.4 \leq x \leq 0.9$) are much enhanced as the system approaches the metal-insulator phase boundary from the metallic side.[18] A similar behavior has been observed in the vicinity ($x=0.05$) of the metal-insulator phase boundary in the analogous system $La_{1-x}Sr_xTiO_3$ and is interpreted as a critical enhancement of density of states at E_F or carrier mass due to the strong correlation.[19] For the case of $La_{1-x}Sr_xTiO_3$, the same conclusion was also obtained by measurements of the electronic specific heat[19] and optical conductivity spectra.[20] Similarly in $Y_{1-x}Ca_xTiO_3$, the T-linear coefficient (γ) of the low-temperature specific heat[21] was observed to increase in a parallel manner with χ. This indicates that the observed enhancement in χ is mostly due to an increase of the carrier mass and least to the Stoner-type enhancement, as far as the metallic phase for $x \geq 0.4$ is concerned.

The $x=0$ ($YTiO_3$) and $x=0.1$ crystals undergo the ferromagnetic transition around 25 and 10 K, respectively, which was revealed by the magnetization measurement in a weak magnetic field (10 mT).[22] However, the samples with $x \geq 0.2$ show no spin-ordered phase, at least down to 5 K. In Fig. 3(b), the inversed susceptibility is plotted against temperature for the samples with $x \leq 0.35$. The data for the $x=0$ and 0.1 samples obey the Curie-Weiss law with the Weiss temperatures, 25 and 10 K, respectively, which agree well with the critical temperatures (T_c's) for those ferromagnetic samples. With increasing x above 0.1, the χ^{-1} value increases while maintaining its slope against temperature. In other words, the apparent negative Weiss temperature obtained by an extrapolation (a straight line in the figure) from the high-temperature behavior tends to increase in an absolute magnitude. This may not necessarily mean that the nature of the exchange interaction between the Ti spins changes from ferromagnetic to antiferromagnetic with hole doping, but should be rather interpreted as signaling a transitional behavior from the localized to itinerant character of the electron states.[23] In the $x=0.30-0.35$ samples near the insulator-metal phase boundary, the low-temperature behavior of χ appears to be governed by presence ($\sim 15\%$) of localized Curie spins.

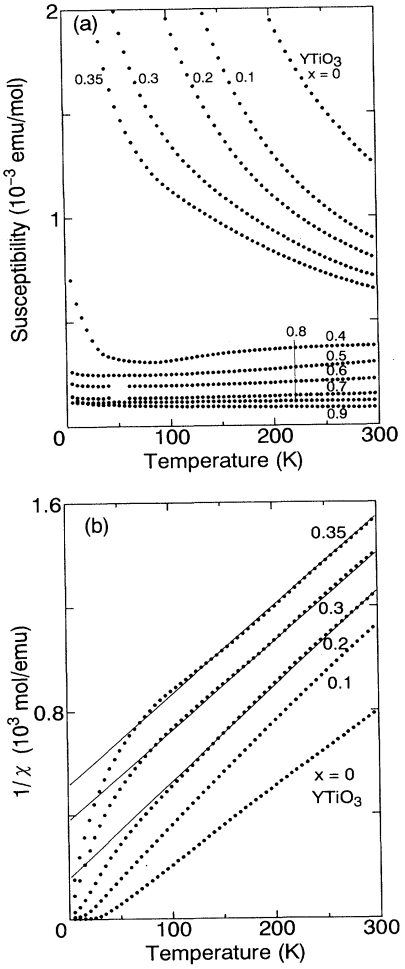

FIG. 3. Temperature dependence of (a) magnetic susceptibility and (b) inversed magnetic susceptibility in $Y_{1-x}Ca_xTiO_3$. Applied magnetic field was 1 T and the data are corrected for diamagnetic contribution arising from the ionic cores.

IV. OPTICAL SPECTRA

We show in Fig. 4 spectra of optical reflectivity in $Y_{1-x}Ca_xTiO_3$ at room temperature (~ 295 K) in the photon-energy region from 0.0075 to 20 eV. In the insulating or semiconducting samples with $x \leq 0.3$ and $x \geq 0.9$, prominent phonon structures appear in the infrared region. In the parent compound $YTiO_3$ ($x=0$), nine optical-phonon modes are observed below 0.1 eV, which are all expected for the $GdFeO_3$-type structure.[24] As an indication of the lowest electronic transition, a broad hump is barely discernible at 1.0–1.5 eV in $YTiO_3$, which is followed by the structures due to the interband transitions lying above 4 eV.

With increase of x, the infrared phonon structures are gradually diminished or blurred and a high reflectance band stands out accompanying an apparent plasma edge around 1 eV. Even in typically metallic samples with $x=0.6$ or 0.8, however, the phonon structures overlapping the plasmalike high reflectance band are still discernible. This may indicate a poor screening effect by carriers perhaps due to the narrow $3d$ electron band with strong correlations. With increasing x above 0.6 or equivalently decreasing the band filling $n(=1-x)$ below 0.4, the plasma edge in the metallic phase was observed to shift to lower energy, which is obviously ascribed to a decrease in the carrier density. In the end compound $CaTiO_3$ with no d electron shows no electronic transition below 4 eV apart from the optical-phonon structures. (The high reflectance band in the far-infrared region in $CaTiO_3$ is due to the soft phonon mode and should not be confused with the plasmalike metallic response.)

We show in Fig. 5 spectra of the optical conductivity $\sigma(\omega)$ below 7 eV, which were derived by the aforementioned procedure of the Kramers-Kronig analysis of the corresponding reflectivity data. First, let us focus on the

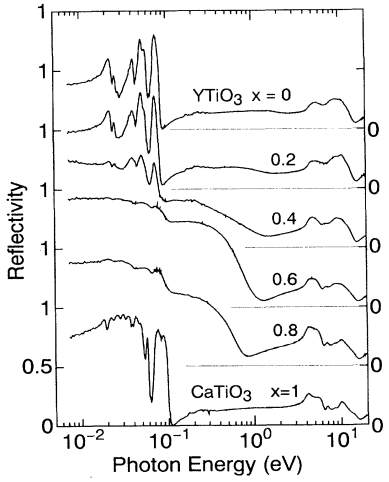

FIG. 4. Reflectivity spectra in $Y_{1-x}Ca_xTiO_3$ at room temperature.

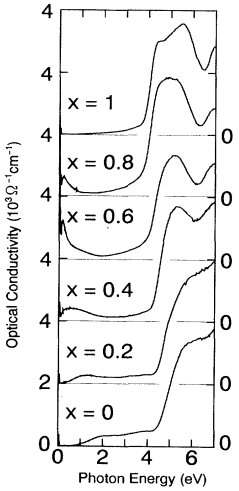

FIG. 5. Optical conductivity spectra in $Y_{1-x}Ca_xTiO_3$ at room temperature.

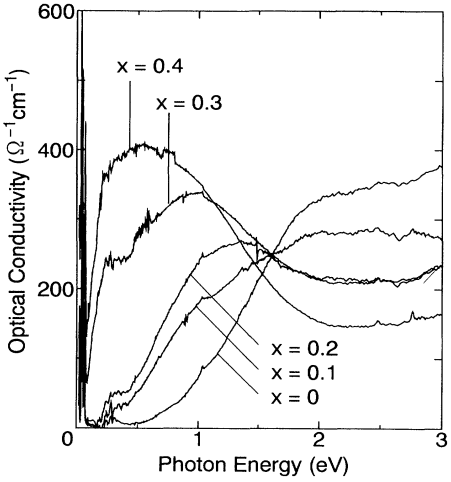

FIG. 6. Optical conductivity spectra for nonmetallic or barely metallic samples of $Y_{1-x}Ca_xTiO_3$ below 3 eV.

$\sigma(\omega)$ spectrum in the parent Mott-Hubbard insulator $YTiO_3$, which is shown in the bottom of Fig. 5. In $YTiO_3$ ($x=0$), onset structures are observed in the $\sigma(\omega)$ spectrum at ~ 0.8 and 4.3 eV. Judging from their energy positions and spectral intensity as well as their x-dependent features (*vide infra*), the former transition can be assigned to the Mott-Hubbard-gap transition between the lower and upper Hubbard bands ($3d$ states), while the latter to the charge-transfer- (CT) type excitations from the occupied O $2p$ states to the upper Hubbard band. In this context, the $\sigma(\omega)$ spectrum below ~ 6 eV essentially reflects the profile of the density of states for the occupied states where zero of the photon energy corresponds to the lower edge of the upper Hubbard band. The Mott-Hubbard-gap transition is relatively weak in intensity as compared with the CT-type p-d transition.

With hole doping, the onset arising from the Mott-Hubbard-gap transition appears to shift to lower energy accompanying the peak structure in the midinfrared region (0.2–0.4 eV). Such a midinfrared $\sigma(\omega)$ peak survives in the typically metallic region ($0.4 \leq x \leq 0.8$) associated with a Drude tail in the lower-energy region (<0.1 eV). (Detailed description and discussion about the low-energy structures in the $\sigma(\omega)$ spectra will be given in Sec. V using the figures in a magnified scale.) On the other hand, the absorption onset of the $2p$-$3d$ transition also shifts to lower energy with hole doping, e.g., from 4.3 eV in $YTiO_3$ ($x=0$) to 3.6 eV in $CaTiO_3$ ($x=1$). This is partly due to a shift of the Fermi level with decreasing the band filling and partly due to the level shift of the O $2p$ states arising from a change of the Madelung-type electrostatic potential.[25]

V. CHANGE OF ELECTRONIC STRUCTURES WITH HOLE DOPING

In order to see a change of the electronic states near the Fermi level with hole doping, we show in Fig. 6 the $\sigma(\omega)$ spectra below 3 eV for the hole-doping region ($0 \leq x \leq 0.4$) where the compounds are nonmetallic or barely metallic. The Mott-Hubbard-gap transition arises around 0.8 eV. The value of Mott-Hubbard gap is estimated to be 1.0–1.3 eV, since the low-energy tail of $\sigma(\omega)$ in $YTiO_3$ is likely due to the presence of a few carriers arising from a slight nonstoichiometry in the sample.[22] With hole doping the absorption onset is observed to shift to lower energy. In accord with this, the spectral weight appears to be transferred from the higher-energy region (≥ 1.5 eV). As a result the midinfrared absorption shows a $\sigma(\omega)$ maximum, whose energy position also shifts to lower energy with hole doping as seen in Fig. 6 (and also in Fig. 7). Notably, the isosbetic point is observed at 1.6 eV against hole doping, indicating the one-to-one spectral weight transfer from the higher-lying Mott gap transitions to the lower-lying electronic excitations.

A similar behavior of the spectral weight transfer over a fairly large energy scale has been observed in the $\sigma(\omega)$ spectra of high-T_c cuprates. An important difference from the case of doped cuprates is, however, that there is

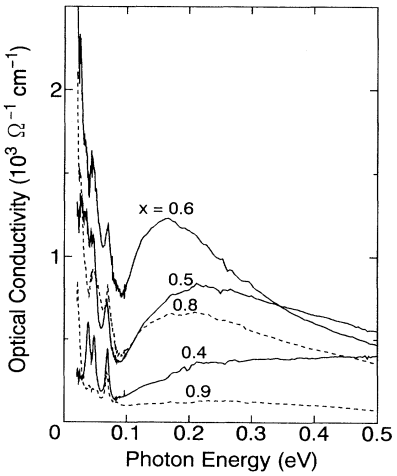

FIG. 7. Optical conductivity spectra for metallic samples of $Y_{1-x}Ca_xTiO_3$.

no clear remnant of the $\sigma(\omega)$ structures around the original band gap in the hole-doped titanates. This is in contrast with the cases of hole- or electron-doped cuprates, e.g., $La_{2-x}Sr_xCuO_4$ (Ref. 6) and $Pr_{2-x}Ce_xCuO_4$ (Refs. 7 and 8) where the $\sigma(\omega)$ feature corresponding to the charge-transfer gap excitations well survives up to $x=0.1-0.15$. Such a difference between the case of doped cuprates and titanates may be due to the different character of the charge gaps in these correlated insulators; i.e., Mott-type vs CT-type.

The $x=0.4$ compound shows a metallic behavior in the transport and magnetic properties as seen in Figs. 2 and 3, yet the $\sigma(\omega)$ spectrum shows a rather sharp drop of the conductivity around 0.2 eV and a Drude tail is hardly discernible. We show in Fig. 7 the details of the low-energy $\sigma(\omega)$ spectra in the metallic phase with $x \geq 0.4$. With increasing x above 0.4, the midinfrared absorption maximum further shifts to lower energy (down to ~ 0.15 eV at $x=0.6\sim 0.8$), yet is still distinguishable from the lower-lying Drude-like tail, which is seen below 0.1 eV together with overlapping phonon structures. Such a pseudogap nature observed even in the metallic region may be ascribed to some localization effect on the narrow $3d$ electron band due to the poorly screened Coulombic potential of the randomly substituted Ca^{2+}/Y^{3+} sites.

In order to estimate the spectral weight transfer to the inner-gap region as well as the weight of the Drude component, we have plotted in Fig. 8 the effective number of electrons $N_{\rm eff}$ measured at 0.1 and 1.0 eV as a function of the hole concentration x (or the band filling $n=1-x$) Here, $N_{\rm eff}$ is defined such as

$$N_{\rm eff}(\omega)=\frac{2m}{\pi e^2 N}\int_0^{\omega}\sigma(\omega)d\omega\ ,$$

N being the number of Ti atoms per unit volume. The specific photon energies, 0.1 and 1.0 eV, were adopted to estimate effective electron numbers which are involved in the Drude-like response relevant to the carrier transport property and in the midinfrared absorption due to the inner-gap states formed within the original Mott-Hubbard gap, respectively. (In plotting $N_{\rm eff}$ as a function of x in Fig. 8, we have assumed a constant phonon contribution (0.0009) and subtracted it from the bare values of $N_{\rm eff}$.)

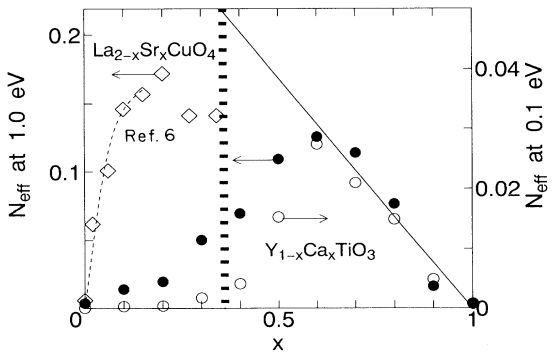

FIG. 8. Effective number of electrons $N_{\rm eff}$ at 0.1 eV (open circles) and 1.0 eV (closed circles) plotted against x. The constant phonon contribution (0.0009) is subtracted from the bare value of $N_{\rm eff}$. To compare the growth of the inner-gap absorption in the present titanate system with the case of the high-T_c cuprates, the result of $N_{\rm eff}$ at 1.0 eV in $La_{2-x}Sr_xCuO_4$ reported by Uchida *et al.* (Ref. 6) is also shown by open diamonds.

According to the plot shown in Fig. 8, the electronic phase in $Y_{1-x}Ca_xTiO_3$ can be divided tentatively to the hole-doping region ($x<0.6$) and electron-doping region ($x>0.6$), where $N_{\rm eff}$ increases with hole doping (x) and with the band filling ($n=1-x$), respectively. In the hole-doping region, the spectral weight of the inner-gap states, $N_{\rm eff}(\hbar\omega=1.0$ eV), readily increases even in the insulating phase below $x \leq 0.3$. By contrast, the value of $N_{\rm eff}(\hbar\omega=0.1$ eV) shows a sharp rise at the nonmetal-metal phase boundary around $x_c \sim 0.35$. These behaviors indicate that the hole doping induces the new states below the original Mott-Hubbard-gap energy but there exists a charge gap larger than 0.1 eV in the nonmetallic phase for $x<x_c$.

It is worth noting here the quantitative difference in the $N_{\rm eff}$ vs x (nominal hole concentration) behaviors for the doped titanate and cuprate compounds. As an example, we have also plotted in Fig. 8 $N_{\rm eff}$ at 1.0 eV as a function of x in $La_{2-x}Sr_xCuO_4$ crystals, which was reported by Uchida *et al.*[6] In $La_{2-x}Sr_xCuO_4$, $N_{\rm eff}$ at 1.0 eV is also a good measure for the estimation of the spectral weight of the inner-gap absorption.[6] $N_{\rm eff}(\hbar\omega=1.0$ eV) in $La_{2-x}Sr_xCuO_4$ (and other cuprate compounds) shows a much steeper rise against the nominal hole concentration x than in $Y_{1-x}Ca_xTiO_3$. This signals that the effective mass of the electrons relevant to the midinfrared absorption (or high-energy optical carrier mass) is much lighter in the doped cuprates. Considering that the charge gap in $YTiO_3$ (~ 1.0 eV) is comparable to or even smaller than that in the undoped cuprate compounds [1.5–2.0 eV (Ref. 26)], the different behavior as seen in Fig. 8 may be attributed to the nature of the charge gap; the Mott gap in the titanates vs CT gap in the cuprates: The Ti $3d$ state character is dominant for the inner-gap states in the $Y_{1-x}Ca_xTiO_3$, whereas the strongly hybridized character of O $2p$ and Cu $3d$ states in the doped cuprate compounds.

In contrast with the case of the hole-doping region, the filling dependence of $N_{\rm eff}$ in the electron-doping region in $Y_{1-x}Ca_xTiO_3$ shows a parallel behavior for $\hbar\omega=0.1$ and 1.0 eV, at least up to $n=0.4$ (down to $x=0.6$). The behavior can be explained by an increase of electron-type carrier density, which should be proportional with the band filling $n(=1-x)$. Judging from the $\sigma(\omega)$ spectra of the plasmalike response (ignoring the details of the pseudogap behavior around 0.1 eV) in the metallic phase (see Fig. 5), $N_{\rm eff}(\hbar\omega=2.0$ eV) is a good measure for estimation of the optical carrier mass. If we assume that the carrier density is given by the band filling n, the linear n dependence of $N_{\rm eff}(\hbar\omega=2.0$ eV) gives the optical carrier mass of $\sim 2.5m_0$. (The present analysis is almost equivalent to the conventional one based on the plasma frequency.) The quantity is comparable with the case in $La_{1-x}Sr_xTiO_3$ for $x>0.5$ (Ref. 20) and with the result of the band calculation for $SrTiO_3$.[27]

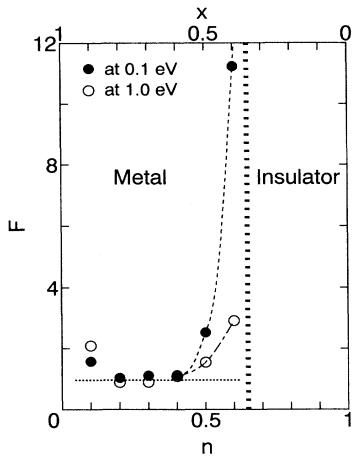

FIG. 9. Mass enchancement factor (F), which was estimated from the value of $N_{\rm eff}(\hbar\omega=0.1$ eV) and $N_{\rm eff}(\hbar\omega=1.0$ eV), as a function of the band filling $n\,(=1-x)$. Closed and open circles are for $\hbar\omega=0.1$ eV and $\hbar\omega=1.0$ eV, respectively.

In the above context, an appreciable decrease in $N_{\rm eff}$ for both $\hbar\omega=0.1$ and 1.0 eV with increasing $n\,(=1-x)$ above 0.4 may be viewed as signaling an increase of the carrier effective mass. This is consistent with the observed increase in the Pauli paramagnetic susceptibility with n in the metallic phase [see Fig. 3(a)]. Quite a similar phenomenon has been observed near the metal-insulator phase boundary ($x_c\sim0.05$) in $La_{1-x}Sr_xTiO_3$ by measurements of optical conductivity spectra, electronic specific heat, and Pauli paramagnetic susceptibility.[19,20] To estimate the mass enhancement from the x dependence of $N_{\rm eff}$ in the present system $Y_{1-x}Ca_xTiO_3$, we may take the ratio (F) of the observed $N_{\rm eff}$ value to the linearly extrapolated one from the low-filling region (as indicated by a straight line in Fig. 8). The mass enhancement factor F, which was estimated by the value of $N_{\rm eff}(\hbar\omega=0.1$ eV) or $N_{\rm eff}(\hbar\omega=1.0$ eV), is plotted against the filling $n\,(=1-x)$ in Fig. 9. The factor F was observed to steeply increase as the system approaches the metal-insulator phase boundary. The enhancement is more appreciable for the $\hbar\omega=0.1$ eV case than for the $\hbar\omega=1.0$ eV case, which is no doubt a consequence of the electron-correlation effect. In accord with the present results, preliminary measurements of the T-linear coefficient (γ) of the low-temperature specific heat in $Y_{1-x}Ca_xTiO_3$ (Ref. 21) have indicated that the renormalized density of states at E_F and hence m^* are significantly enhanced in a similar manner as observed in Fig. 9 as the compound approaches the metal-insulator phase boundary from the metallic side.

VI. CONCLUSION

We have synthesized a system, $Y_{1-x}Ca_xTiO_3$, which can be viewed as a hole-doped Mott-Hubbard insulator in the low-x region and an electron-doped narrow d-band metal in the high-x region. The transition from a Mott-Hubbard insulator to a correlated metal was observed to take place around $x_c\sim0.35=1-n_c$ ($n_c\sim0.65$). In the insulating phase ($x<x_c$), the Curie-Weiss-type temperature dependence of the magnetic susceptibility was observed with a doping-dependent change of the apparent Weiss temperature, which may be interpreted as indicating a crossover of the magnetic properties from the localized to itinerant nature. In the metallic phase ($x>x_c$), a typical Pauli paramagnetic susceptibility was observed, though the value is enhanced near the metal-insulator phase boundary.

Optical measurements have revealed a characteristic change in electronic structures with hole doping or with changing the band filling. In the parent insulator $YTiO_3$ the Mott-Hubbard-gap transition is observed above 0.8 eV. With hole doping the gap appears to shift to a lower energy accompanying a spectral weight transfer from the Mott-gap transition region. In the metallic region, the midinfrared absorption peak survives perhaps due to the poorly screened Coulombic potential of the randomly substituted A sites.

The spectral weight in the far-infrared region below 0.1 eV as well as in the inner-gap region below 1.0 eV was estimated as a function of hole concentration of x (or of the band filling $n=1-x$). The inner-gap states evolve with hole doping but show a charge gap in the insulating phase. On the other hand, the simple behavior of the $3d$ band filling was observed in the n dependence of the spectral weight with a nearly constant effective mass in the low-n (high-x) region. With further filling the $3d$ band up to the vicinity of n_c, however, a critical enhancement of the carrier mass was observed perhaps due to the electron-correlation effect.

The long-range spin order seems to vanish above $x=0.1$ in $Y_{1-x}Ca_xTiO_3$. Therefore, the metal-insulator transition around $x\sim0.35$ in $Y_{1-x}Ca_xTiO_3$ is not simply related to the existence of the magnetically ordered phase, but may be rather characterized by a combined effect of the electron correlation and random potential: As x decreases from the high-x metallic side, the carrier effective mass is enhanced due to the filling-dependent change of the correlation effect and exceeds some critical value, above which the carriers show the localization perhaps due to the random potential mainly arising from the ionic A sites (Y/Ca mixture).

ACKNOWLEDGMENTS

We are grateful to Y. Okada, K. Kumagai, Y. Iye, A. Fujimori, and H. Takagi for enlightening discussions. We are also indebted to K. Tamasaku and S. Uchida and to M. Fujisawa for their help in the far-infrared and vacuum-ultraviolet measurements, respectively. This work was supported by a Grant-In-Aid from the Ministry of Education, Science and Culture, Japan.

*Author to whom correspondence should be addressed.
[1]D. A. MacLean and J. E. Greedan, Inorg. Chem. **20**, 1025 (1981).
[2]D. A. MacLean, K. Seto, and J. E. Greedan, J. Solid State Chem. **40**, 241 (1981).
[3]C. W. Turner, M. F. Collins, and J. E. Greedan, J. Magn. Magn. Mater. **23**, 265 (1981).
[4]F. Lichtenberg, D. Widmer, J. G. Bednorz, T. Williams, and A. Reller, Z. Phys. B **82**, 211 (1991).
[5]J. Zaanen, G. A. Sawatzky, and J. W. Allen, Phys. Rev. Lett. **55**, 418 (1985).
[6]S. Uchida, T. Ido, H. Takagi, T. Arima, Y. Tokura, and S. Tajima, Phys. Rev. B **43**, 7942 (1991).
[7]S. L. Cooper, G. A. Thomas, J. Orenstein, D. H. Rapkine, A. J. Millis, S-W. Cheong, A. S. Cooper, and Z. Fisk, Phys. Rev. B **41**, 11 605 (1990).
[8]T. Arima, Y. Tokura, and S. Uchida (unpublished).
[9]H. Romberg, M. Alexander, N. Nücker, P. Adelmann, and J. Fink, Phys. Rev. B **42**, 8768 (1990).
[10]C. T. Chen *et al.*, Phys. Rev. Lett. **66**, 104 (1991).
[11]D. A. MacLean, Hok-Nam Ng, and J. E. Greedan, J. Solid State Chem. **30**, 35 (1979).
[12]D. A. Crandles, T. Timusk, and J. E. Greedan, Phys. Rev. B **44**, 13 250 (1991); D. A. Crandles, J. D. Garrett, T. Timusk, and J. E. Greedan, Physica C **201**, 407 (1992).
[13]J. D. Garrett, J. E. Greedan, and D. A. MacLean, Mater. Res. Bull. **16**, 145 (1981).
[14]J. P. Goral, J. E. Greedan, and D. A. MacLean, J. Solid State Chem. **43**, 244 (1982).
[15]For a review on the filling control in layered cuprate compounds, see, for example, Y. Tokura and T. Arima, Jpn. J. Appl. Phys. **29**, 2388 (1990).
[16]J. E. Sunstrom, S. M. Kauzlarich, and P. Klavins, Chem. Mater. **4**, 346 (1992).
[17]Y. Okada and Y. Tokura (unpublished).
[18]Y. Tokura, J. Phys. Chem. Solids **53**, 1619 (1992).
[19]Y. Tokura, Y. Taguchi, Y. Okada, Y. Fujishima, T. Arima, K. Kumagai, and Y. Iye, Phys. Rev. Lett. **70**, 2126 (1993).
[20]Y. Fujishima, Y. Tokura, T. Arima, and S. Uchida, Phys. Rev. B **46**, 11 167 (1992).
[21]K. Kumagai, T. Suzuki, Y. Taguchi, Y. Okada, Y. Fujishima, and Y. Tokura, Phys. Rev. B (to be published).
[22]T_c in the $x=0$ sample is rather sensitive to a slight offstoichiometry of the sample, or equivalently to presence of a few hole-type carriers. The $YTiO_3$ which was synthesized in a stronger reducing condition and hence better stoichiometrically showed a slightly higher T_c ($\sim$30 K).
[23]T. Moriya and H. Hasegawa, J. Phys. Soc. Jpn. **48**, 1490 (1980).
[24]M. Couzi and P. Vam Huong, J. Chem. Phys. **69**, 1339.
[25]J. B. Torrance, P. Lacorre, C. Asavaroengchai, and R. M. Metzger, Physica C **182**, 351 (1991).
[26]Y. Tokura *et al.*, Phys. Rev. B **41**, 11 657 (1990); S. L. Cooper *et al.*, *ibid.* **42**, 10 785 (1990).
[27]L. F. Mattheiss, Phys. Rev. B **6**, 4718 (1972).